PET, CT, and MRI in the Evaluation of Neuropsychiatric Disorders: Current Applications

Paul R. Jolles*, Peter R. Chapman†, and Abass Alavi

Division of Nuclear Medicine, Department of Radiology, Hospital of the University of Pennsylvania, Philadelphia, Pennsylvania

Positron emission tomography (PET) is emerging as a very useful clinical tool and is adding a great deal to our understanding of the pathophysiology of central nervous system (CNS) disorders. Although computed tomography (CT) and magnetic resonance imaging (MRI) have had a dramatic impact on patient management, there is often an important associated function abnormality which is best assessed by PET. In normal aging and in dementia, the CT and MRI brain changes of atrophy and white matter abnormalities are frequently nonspecific. PET has been more diagnostic, showing characteristic regional metabolic abnormalities. Evaluation of brain tumors such as astrocytomas with PET has demonstrated better correlation with histologic grade compared to CT. Unlike CT or MRI, PET can help to distinguish radiation necrosis from recurrent tumor, and can differentiate the extent of metabolically active tumor from surrounding edema. PET is useful in evaluating stroke patients, providing better prognostic information and demonstrating abnormalities sooner than CT. In epilepsy, PET appears to be superior to MRI in localizing seizure foci in patients with partial seizures. In head trauma patients, metabolic patterns are being described which will likely have an effect on patient management. The use of PET in schizophrenia has yielded very interesting results, with common patterns of metabolic abnormalities being demonstrated. CT and MRI in these patients have not been very useful. PET has also shown promise in movement disorders such as Huntington's disease. It is now clear that PET is already clinically useful and can provide valuable information unobtainable by CT and MRI. As new radioligands are developed, PET is certain to assume an even more important role in the future.

J Nucl Med 30:1589–1606, 1989

The past two decades have been witness to remarkable progress in our understanding of brain structure and function, with advances in anatomic and functional brain imaging playing a major role. Computed tomography (CT) and, more recently, magnetic resonance imaging (MRI) have provided exceptional anatomic detail. However, these modalities are unable to assess the global or regional functional status of the brain. It is well known that virtually all abnormalities affecting the brain have a functional component, sometimes in the absence of an anatomic lesion. Today, brain function is best evaluated with positron emission tomography (PET). Although lacking the resolution of CT or MRI, the advantage of PET over the anatomic imaging modalities is that biologically important atoms such as nitrogen and carbon can be incorporated into novel compounds which allow mapping of regional brain function and metabolism (Fig. 1). The capabilities offered by PET enable researchers to measure and image regional blood flow, oxygen and glucose metabolism, protein synthesis, and neurotransmitter/neuroreceptor systems. With PET now moving from the research laboratory into the clinical nuclear medicine arena, we have indeed entered a new era in brain imaging. This paper will deal with the application of PET, CT, and MRI as currently used in the clinical evaluation of common brain abnormalities.

Received May 19, 1989; revision accepted May 31, 1989.

For reprints contact: Abass Alavi, MD, Div. of Nuclear Medicine, Dept. of Radiology, Hospital of the University of Pennsylvania, Philadelphia, PA 19104.

*Present address: Department of Radiology, University of Arkansas for Medical Sciences, 4301 West Markham St., Little Rock, Arkansas 72205.

† Present address: Nuclear Medicine & Ultrasound Associates, P.O. Box 6, Westmead. NSW 2145, Australia.

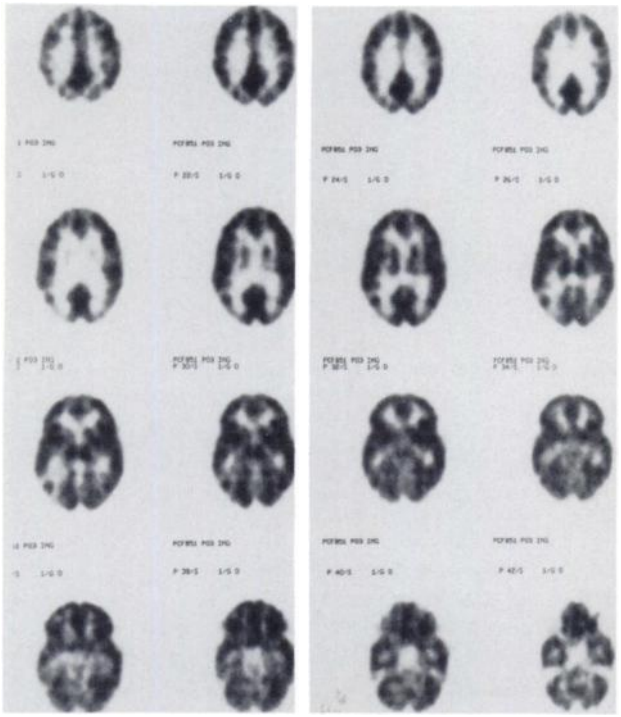

FIGURE 1
Representative transaxial images from an FDG-PET study of a young, normal subject are shown from the level of the high convexity (upper left) to the cerebellum (lower right). Note that the cortical and subcortical structures are well-delineated, and appear relatively symmetric between hemispheres.

AGING AND DEMENTIA

Evaluation of the brain in aging and dementia has been extensive, with functional imaging (PET) appearing to have greater sensitivity in detecting early regional changes than CT or MRI. In the normal elderly population, pathologic studies have reported regional neuron loss in the frontal, parietal and temporal lobes (*1–3*). Typical changes seen on anatomic imaging in these individuals include generalized ventricular enlargement and cortical sulcal atrophy; of these findings, sulcal atrophy and the width of the third ventricle appear to be better correlated with aging using CT (*4–6*). Both MRI and CT demonstrate the ventricular system quite well, with MRI being superior to CT in delineating the cortical sulci due to lack of beam hardening artifacts.

White matter abnormalities are also common in the healthy elderly subject, manifesting as periventricular and/or focal deep white matter hyperintensities on MRI, or hypodensities on CT. MRI is the more sensitive in detecting these lesions (*7*). Although there is general agreement that the occurrence of white matter abnormalities increases with age (*8,9*), the actual underlying pathologic mechanism is controversial. Most reports conclude that these abnormalities represent areas of hypoperfusion or infarction, with hypertension found to be a common underlying condition (*10,11*). However, the same changes have been found in subjects without hypertension or other identifiable vascular risk factors (*12*), and it is possible that several etiologies may be involved. Our preliminary data suggest that deep white matter lesions do not have a significant effect on regional or global metabolic rates.

The findings seen on PET in normal aging are somewhat controversial. Several investigators have reported that there is probably no significant decrease in whole brain glucose metabolism using fluorine-18 (^{18}F) fluorodeoxyglucose (FDG) (*13–15*), although there are other reports showing a decline (*16,17*). However, a number of investigators have described diminished regional glucose metabolism in healthy elderly subjects in the temporal, parietal, somatosensory, and especially the frontal regions (*17–21*). Relative preservation of posterior metabolism (particularly in the calcarine cortex) has also been reported (*20,21*). A summary of our regional metabolic data in normal aging is presented in Table 1.

Whether or not there is a definite decrease in cerebral blood flow (CBF) or cerebral oxygen metabolic rate ($CMRO_2$) as measured by PET has not been established. Some workers have described no change with normal aging using the nitrous oxide CBF technique (*16,22*); others have reported diminished CBF and/or $CMRO_2$ (*23–26*). Although controversial, these findings suggest that there may be regional abnormalities in cerebral metabolism in normal aging using PET.

There has been much interest in evaluating the changes which occur in the brain in the dementing disorders. The most common cause of dementia is Alzheimer's disease (AD), which accounts for at least half of the cases. Other causes include multiple infarctions (multi-infarct dementia) (MID), AD, and MID in combination, and other less common etiologies such as normal pressure hydrocephalus, mass lesions, infections, AIDS, and metabolic/nutritional disorders (*27–30*).

The CT and MRI findings in AD include ventricular and cortical sulcal enlargement, which are more pro-

TABLE 1
Significant Regional Hypometabolism: Individual ROIs*

Frontal	Temporal
Anterior corpus callosum	Middle temporal gyrus
Cingulate gyrus	
Frontal eye fields	Parietal
Frontal pole	Superior parietal lobule
Middle frontal gyrus	
Sensorimotor	
Primary sensory cortex	

* 59 ROIs in each hemisphere (118 comparisons by two-tailed t-test [young vs. older controls]).
ROIs significant at $p = 0.001$.
[Reprinted with permission Ref. (*15*)].

nounced than those seen in normal aging (*31–33*). However, these findings are not specific for AD and may be found in many other types of nondementing brain disorders. Focal temporal lobe atrophy with enlargement of the surrounding cerebrospinal fluid (CSF) space has been described in AD patients using CT (*34*); thus far, this appears to be the only anatomic imaging finding reported which is said to distinguish AD patients from normal elderly subjects with an 80–90% accuracy. White matter disease has also been described in AD patients. At present, there is much debate in the literature as to whether AD patients have a greater degree of white matter abnormality compared to normal elderly controls. Overall, the data suggest that AD patients and normal controls cannot be reliably distinguished by the number of focal deep white matter lesions. However, the presence of certain patterns of periventricular hyperintensity (PVH) on MRI might aid in making this distinction. Fazekas et al. (*12*) have described a halo of PVH which was seen in six of 12 AD patients, but not in controls or MID patients. Normal elderly subjects had caps, pencil-thin, or absent PVH. Additional studies may help to clarify the diagnostic significance of these findings. Patients in this study with MID tended to have extensive focal and confluent white matter abnormalities, associated with "classical" infarcts.

Phosphorus-31 magnetic resonance spectroscopy of the brain has been used to evaluate AD patients (*35,36*). However, no findings unique to AD have yet been described; our own preliminary data showed no significant differences between AD patients and controls (*37*).

The use of FDG PET in dementia shows promise, as several types of dementing disorders have been reported to demonstrate characteristic metabolic patterns. A number of studies (*21,38,39*) have described diminished regional glucose metabolism in AD patients in the parietal and temporal lobes; the frontal lobes may also demonstrate hypometabolic changes, particularly in severe cases (Fig. 2). Relatively preserved glucose metabolism has been noted in the primary visual and sensorimotor cortices, as well as the cerebellum (Fig. 3). The visual cortex glucose metabolism especially remains quite stable during different stages of AD. Because of this observation, we usually use the visual cortex metabolic rates for normalization rather than that of the cerebellum as described in the literature. These data are presented in Table 2.

Hemispheric asymmetry may also be present, with more severe hypometabolism on the left compared to the right; this may explain the language difficulties seen in certain advanced AD patients. Global and regional $CMRO_2$ was reported to be decreased in AD patients, especially in the temporal and parietal regions; substantially diminished frontal oxygen metabolism has been noted in severe cases. An associated decrease in CBF

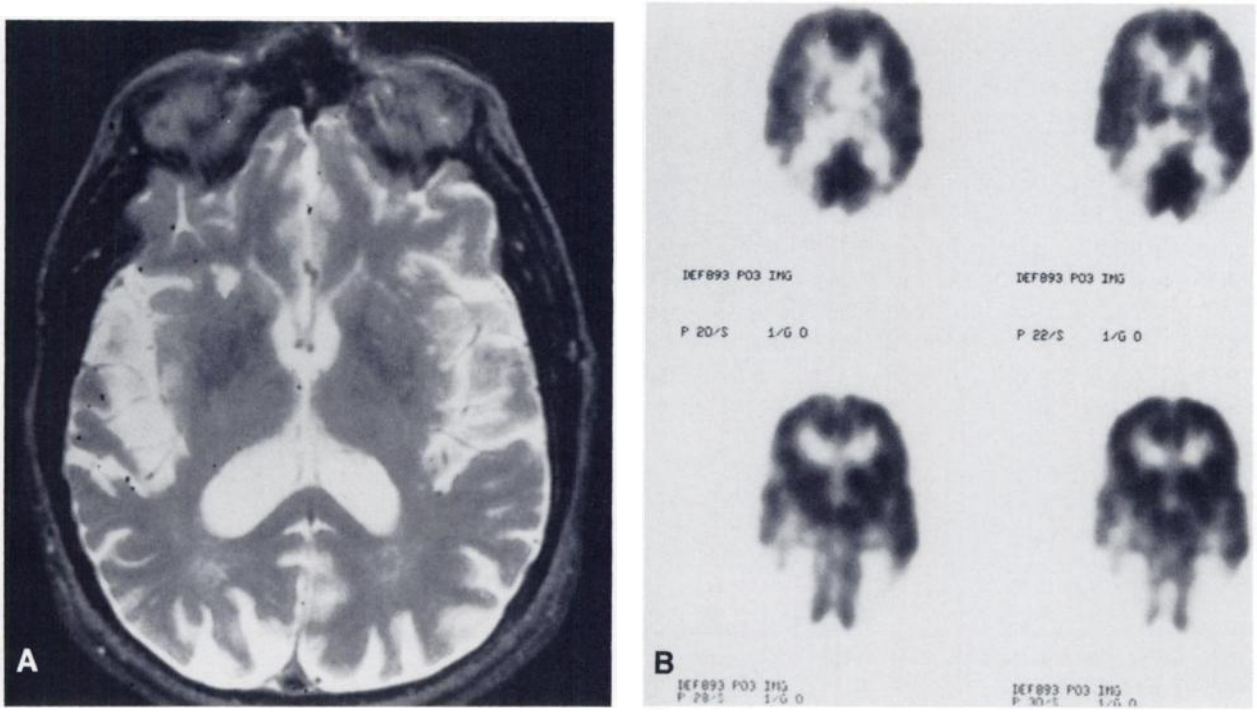

FIGURE 2
A: The MRI image of a moderately early Alzheimer's disease patient shows significant bilateral cortical atrophy and ventricular enlargement. There are also a few foci of deep white matter hyperintensity. B: The FDG-PET image shows profound bilateral parieto-occipital hypometabolism with additional abnormality in the right temporal lobe. The remainder of the cortical and subcortical structures are relatively intact.

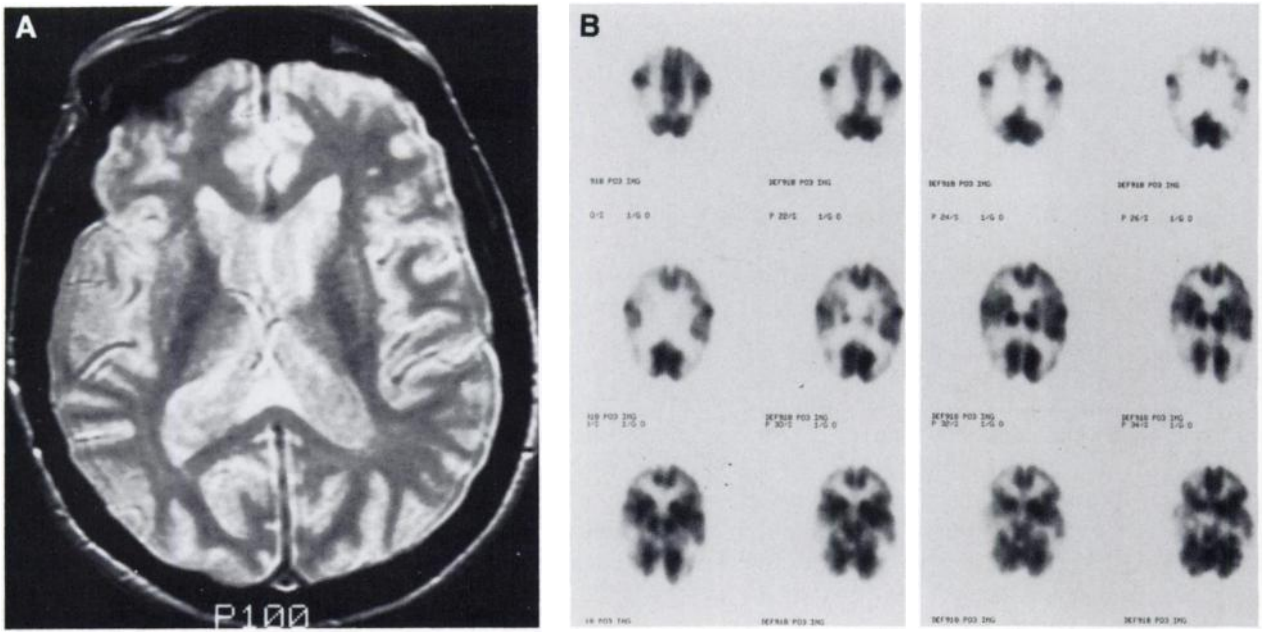

FIGURE 3
A: MRI image of a patient with advanced Alzheimer's disease shows mild cortical atrophy and moderate ventricular enlargement, with a few foci of deep white matter hyperintensity. These findings are nonspecific and are frequently seen in elderly individuals. B: Sequential FDG-PET images show marked bilateral parieto-occipital hypometabolism and moderate bilateral fronto-temporal hypometabolism. There is preservation of glucose metabolism in the sensorimotor and calcarine (primary visual) cortices, and in the subcortical nuclei, frequently noted in Alzheimer's disease.

has also been reported (*41*,*42*). AD patients with a progressive decrease in glucose metabolism have been shown to display corresponding cognitive loss. In addition, regions of local hypometabolism were reported to correspond to areas of cortical neuronal loss in AD (*43*).

With PET, other types of dementia may be able to be distinguished from AD. MID patients tend to demonstrate scattered focal regions of diminished glucose metabolism (*44*), rather than the predominantly diminished parietal and temporal metabolism seen in AD. This finding, along with the characteristic appearance of multiple lesions on MRI (especially in the white matter), establishes the diagnosis in most patients. Individuals with Pick's disease have been reported to exhibit more profound glucose hypometabolism in the frontal regions than in the parietal and temporal regions (*45*). The PET findings seen in demented patients with Huntington's disease and Parkinson's disease will be discussed in the section on movement disorders.

It is clear that PET has the potential to characterize and further our understanding of the various types of dementia. A number of controversies exist, as discussed above. In addition to these, a standardized method for quantification of metabolic data has yet to be achieved; also, the need for atrophy correction of metabolic rates is being recognized (*46*). As these problems are addressed and solved, and selective brain stimulation/activation studies are utilized, great progress in this area will be made.

TABLE 2
Normalization of Quantitative Metabolic Data

Structures used to normalize	Sensitivity	Specificity	Test accuracy	Predictive values positive	Predictive values negative
Calcarine cortex	89%	81%	84%	72%	93%
Cerebellum	100%	57%	72%	56%	100%
Caudate nucleus	5%	78%	52%	12%	60%
Sensorimotor cortex	59%	91%	80%	79%	80%
Whole brain	35%	79%	63%	48%	69%

[Reprinted with permission Ref. (*40*)].

BRAIN TUMORS

Since the mid 1970s, rapid advances in high resolution anatomic imaging have favored the use of CT and MRI (in recent years) for brain tumor characterization. In general, both CT and MRI provide excellent delineation of brain tumors. However, MRI has been reported to be more sensitive than CT due to better resolution, lack of beam hardening or streak artifacts, and multiplane imaging capability. In particular, MRI is superior in evaluating the cerebellum and brainstem, where there may be severe beam hardening artifacts on CT. CT, however, is much superior to MRI in detecting small foci of calcification (*47–50*), which may be seen in lesions such as meningiomas and oligodendrogliomas. Before the introduction of paramagnetic contrast agents such as gadolinium-diethylenetriaminepentaacetic acid ([Gd]DTPA), CT with iodinated contrast was reported to differentiate tumor from surrounding edema much better than MRI. However, this may no longer be the case except for lesions such as lower grade gliomas, which show less reliable enhancement (*51*) but generally do not cause significant edema.

The following discussion will center upon astrocytomas, which are common brain tumors. Astrocytomas are generally classified into four grades: Grades I and II (low grade) and Grades III and IV (high grade). By and large, the tumor appearance on CT or MRI corresponds with the histologic grade. On CT, low grade tumors typically present as hypodense lesions with little if any mass effect or surrounding edema. Contrast enhancement is infrequent and, if present, is usually inhomogeneous. The tumor borders may be well defined, although local infiltration may result in a less distinct margin. Calcification (usually central) may be present. These lesions appear as high signal intensity regions on T2-weighted MR images, and low signal intensity on T1-weighted images. Again, as on CT, little mass effect or edema is evident, and enhancement with [Gd]DTPA is variable. Punctate calcifications will probably not be detected on MRI, although large calcifications may be delineated (*52–53*). High grade tumors typically appear as irregular, inhomogeneous density lesions on CT with associated mass effect, surrounding edema, and contrast enhancement. On MRI, these lesions demonstrate high (or inhomogeneous) signal intensity on T2-weighted images with associated edema, mass effect, and contrast enhancement with [Gd]DTPA(*50*).

Although CT and MRI usually provide excellent delineation of brain tumors when they are originally diagnosed, a significant clinical dilemma arises in patients who have received radiation therapy. Unfortunately, neither imaging modality is able to distinguish recurrent tumor from radiation necrosis (*54*). This is an area where PET can provide a valuable contribution.

The use of positron emitting radiopharmaceuticals in the evaluation of brain tumors is not a new application; Wrenn et al. described a scintillation counter for this purpose in 1951 (*55*). Since the advent of modern PET scanners, large numbers of brain tumors have been evaluated, mainly with FDG; ^{11}C L-methionine (reflecting neutral amino acid transport) (*56*) and ^{11}C putrescine (*57*) have also been employed. In most cases, high grade tumors appear hypermetabolic, while low grade tumors are hypometabolic (Figs. 4 and 5). Associated edema, cystic changes, and necrosis also manifest as hypometabolic regions. Overall, the data show a striking correlation between PET findings and histologic grade, with PET being more accurate in predicting degree of tumor malignancy than CT. PET was also reported to be of better prognostic value than CT in predicting

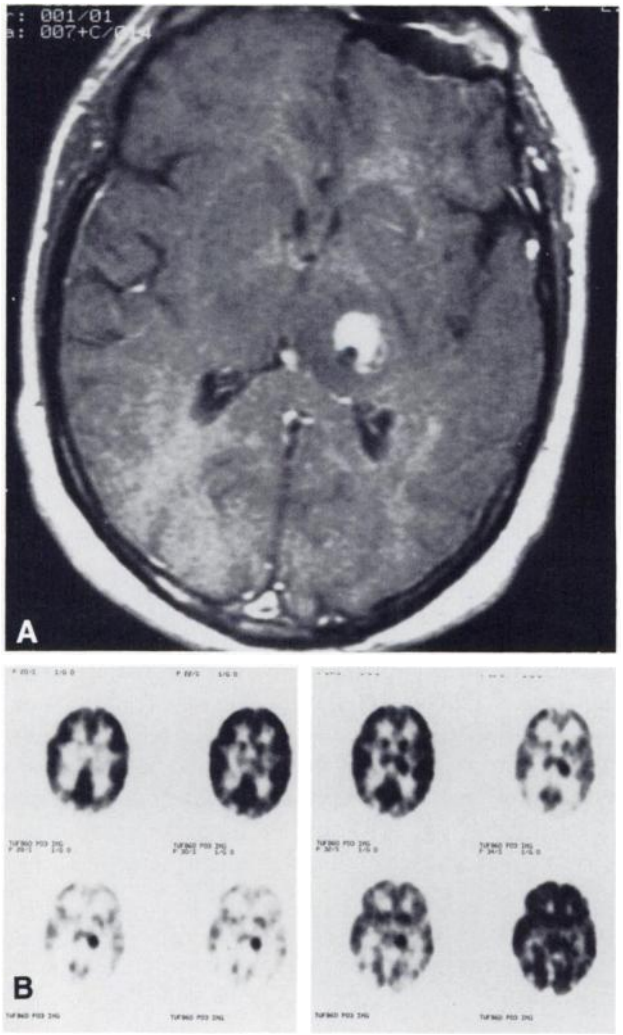

FIGURE 4
A: The selected MR image of a left thalamic lymphoma demonstrates tumor enhancement with gadolinium-DTPA. A small low signal intensity region is seen within the mass, representing hemorrhage. There is only mild mass effect. B: The FDG-PET images show a focal hypermetabolic focus in the left thalamus, consistent with a very active tumor. Note that there is no surrounding hypermetabolic zone, which suggests the absence of significant edema.

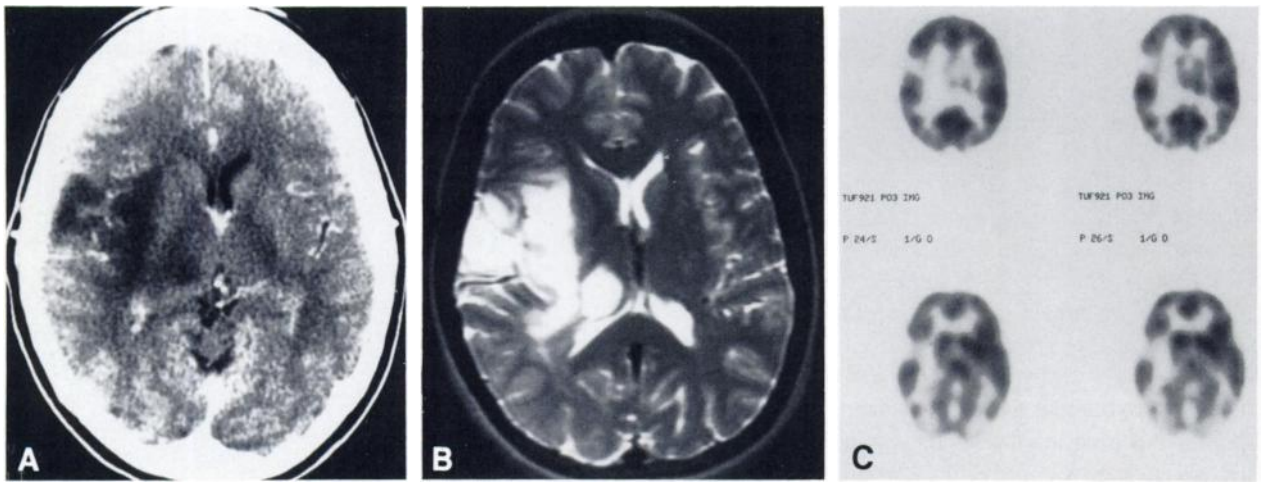

FIGURE 5
A: CT scan in a patient with a low-grade glioma shows an irregular hypodense region in the right temporo-parietal region, involving both the cortex and deep white matter and extending into the region of the right thalamus. There is mild mass effect but no significant contrast enhancement is demonstrated. B: The MR image shows a region of high signal intensity corresponding to the abnormalities seen on the CT scan. Mild mass effect is also noted. C: The FDG-PET images show marked hypometabolism in the right parietal lobe, extending into the temporal lobe. These findings are usually noted in low-grade tumors.

survival in patients with high grade gliomas (*58–62*). Metabolic abnormalities distant from solitary supratentorial lesions have been noted, particularly in the contralateral cerebellar hemisphere (*63*). This phenomenon has been termed "crossed cerebellar diaschisis" by Baron (*64*). Data from our laboratory suggest that ipsilateral hypometabolism may be a remote effect of edema (*65*).

Unlike CT or MRI, PET has been shown to distinguish radiation necrosis from tumor recurrence using FDG (*66, 67*) and ^{11}C L-methionine (*56*), and appears to be the only imaging modality currently able to do so. As might be expected, an area of radiation necrosis appears as a hypometabolic area, and recurrent tumor as a hypermetabolic region (Fig. 6). This feature alone would make PET a valuable and unique tool in helping plan the management of these patients. Some investigators have advocated the use of three dimensional correlation of CT, MRI, and PET images in radiation therapy planning to better define the target volume (*68*).

STROKE

Advances in anatomic and functional imaging have significantly furthered our understanding of the pathophysiology of brain ischemia and infarction. Immediately following cerebral arterial thrombosis or embolic event, hypoperfusion of the brain in the involved arterial distribution occurs. At this stage of an ischemic infarction, there is typically no abnormality seen on noncontrast CT. Approximately 12–24 hr after the ictus, an ill-defined hypodensity is frequently noted, and mass effect due to edema may be present (*69*). However, some authors have reported CT findings which may make it possible to detect ischemic infarction earlier than 12 hr: increased density in a cerebral vessel secondary to an embolus or thrombus (*70*), lower peak amplitude (in Hounsfield Units) of the affected hemisphere on dynamic scanning (*71*), and partial disappearance of the lentiform nucleus in patients with embolic infarction of the middle cerebral or internal carotid artery distribution (*72*). Later on in the course of the infarction, the affected area may become isodense on CT, and then proceed through a stage of contrast enhancement, termed "luxury perfusion". Finally, the end stage of chronic infarction is reached, manifested as an area of well-defined hypodensity associated with enlargement of the adjacent CSF space.

Although there are cases in which CT is able to detect early ischemic infarction, MRI has been reported to be more sensitive overall, showing abnormalities at 1–2 hrs after the ictus in animal studies (*73*). The typical appearance is an area which is of low signal intensity on T1-weighted images and high signal intensity on T2-weighted images, resulting from increased regional water accumulation due to edema. In the chronic stage, the infarct appears as a cyst-like CSF-intensity region. MRI can distinctly demonstrate hemorrhagic infarcts, which may be missed on CT. While CT and MRI provide valuable information on ischemic infarction, PET is better able to track the actual sequence of pathophysiologic events, particularly in the early stages.

PET has been reported to demonstrate abnormalities earlier than CT, and often the metabolic abnormalities are more extensive than would be predicted by CT or MRI. In addition, the abnormal metabolic pattern seen on PET has been related to the type of clinical syndrome, and also to the degree of eventual recovery (*74*, *75*) (Fig. 7).

Using $^{13}NH_3$ and ^{15}O-labeled agents, PET is able to monitor cerebral blood flow and oxygen metabolism in

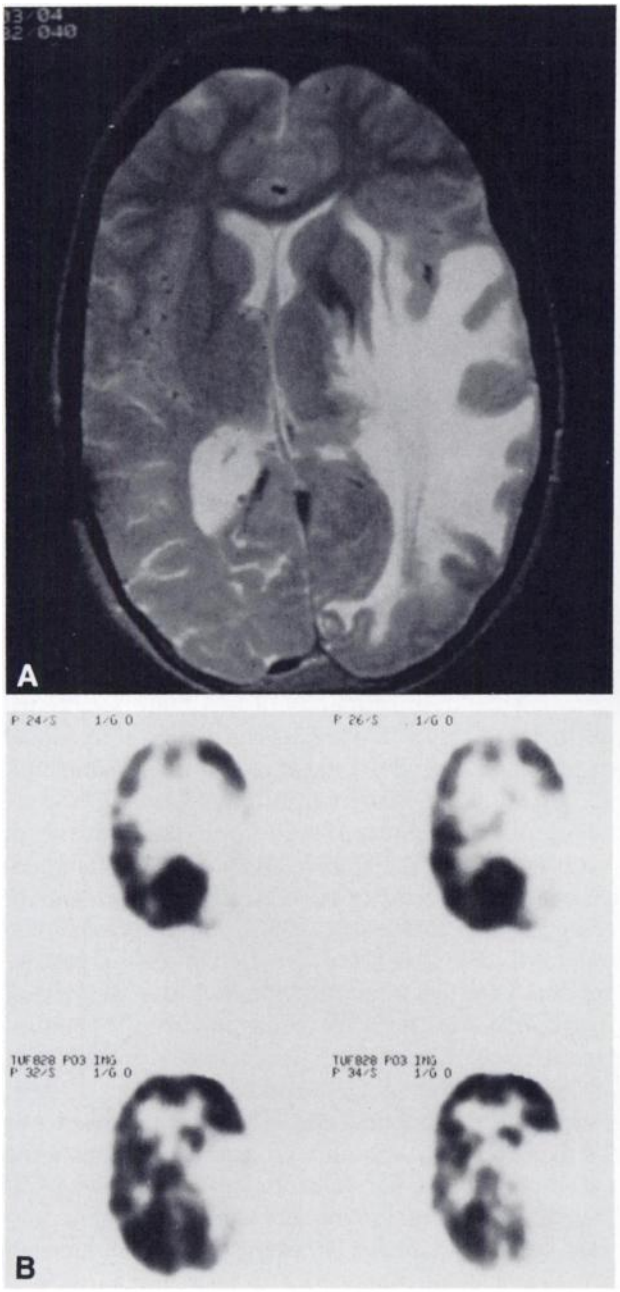

FIGURE 6
A: This brain tumor patient who was studied after radiation therapy demonstrates a large high signal intensity abnormality on MRI in the left parieto-occipital region, with associated mass effect and edema. This MR appearance may be seen with either tumor recurrence or radiation necrosis. B: FDG-PET images show an extensive hypometabolic abnormality in the same region as the MRI scan. These findings are consistent with radiation necrosis rather than recurrent tumor. (With permission: Jolles PR, Chapman PR, Alavi A. Determination of regional cerebral function and structure using computed tomography, magnetic resonance imaging and positron emission tomography. *Adv Func Neuroimag* 1989;2:7–15).

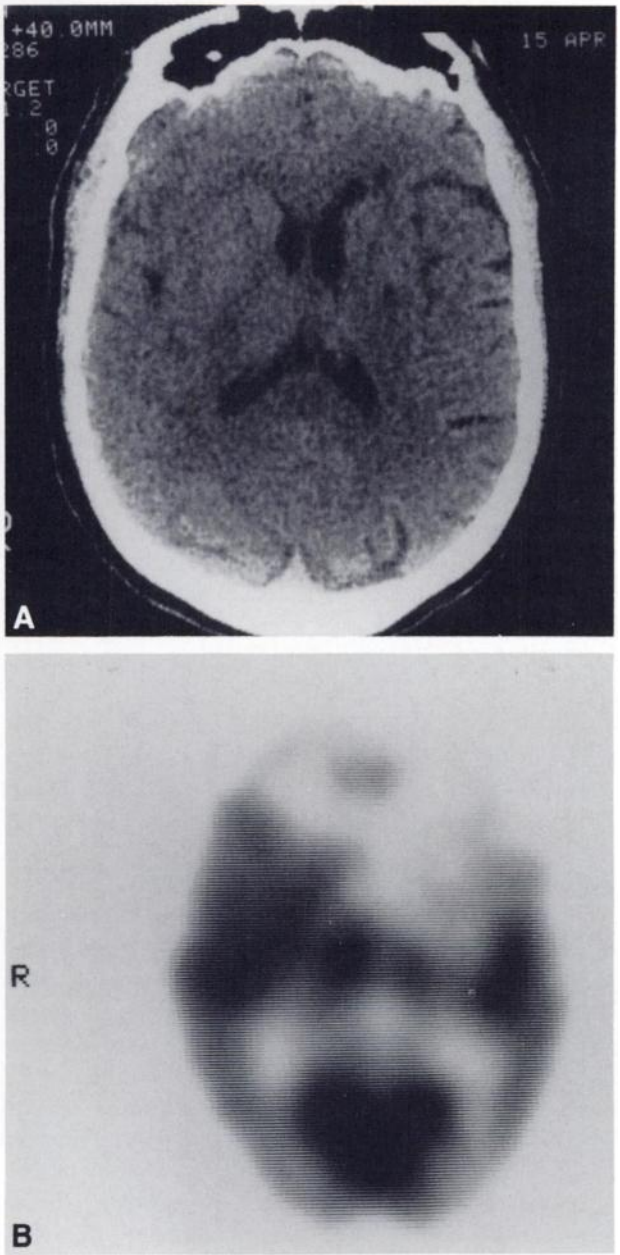

FIGURE 7
A: Noncontrast-enhanced CT image of a patient with a left basal ganglia infarct shows a small hypodense region extending anteriorly from the superior aspect of the head of the left caudate nucleus. Cortical atrophy is present, particularly on the left. B: The FDG-PET image reveals marked hypometabolism in the region of the left basal ganglia, as well as bifrontal hypometabolism. Note the more extensive abnormalities seen on PET compared to CT.

stroke patients. As may be expected in early infarction, local cerebral blood flow (LCBF) decreases; there is a concomitant rise in the local oxygen extraction fraction (LOEF) in an attempt to deliver the maximal amount of oxygen to the compromised region of brain. As the stroke evolves to the "luxury perfusion" stage, LCBF typically increases compared to LOEF (*76*). However, groups of transient ischemic attack (TIA) and stroke patients, some with occlusion of a carotid artery, have been described with diminished LCBF at this stage; this has been termed "misery perfusion" (*77*). Currently, it is not certain whether these patients are at increased risk for infarction (*78, 79*); one patient presenting with a TIA and "misery perfusion" syndrome on PET was described recently, who progressed to an infarction (*80*). Areas of chronic infarction tend to exhibit diminished LCBF and oxygen/glucose metabolism.

Additional hypometabolic foci distant from a cerebral infarction are often noted on PET studies, typically in the absence of corresponding CT or MRI abnormalities (*75, 81*). These may occur in the ipsilateral or contralateral cerebral hemisphere, or may be seen in the contralateral cerebellar hemisphere; the latter was termed "crossed cerebellar diaschisis" (*64*). These abnormalities imply the interruption of crossing pathways in the brain (*63*), and can be seen with other supratentorial abnormalities such as brain tumors and head trauma.

Phosphorus-31 magnetic resonance spectroscopy (MRS) has been used in the investigation of chronic ischemia infarctions in humans (*82*). No findings specific for infarction were described. Further research is required to determine the diagnostic utility of MRS in stroke.

HEAD TRAUMA

The development of CT has had a dramatic impact upon the diagnosis and management of patients with head trauma. More recently, MRI has been shown to be superior to CT in all clinical settings except in acute head trauma (*83*) where CT remains the modality of choice in the diagnosis of surgically correctable lesions (*84*). CT is superior in detecting subarachnoid hemorrhage (*83*) and bony fracture, and in differentiating acute parenchymal hemorrhage from edema. Evaluation is slower and logistically more complex with MRI, particularly with patients on life-support systems. MRI is increasingly becoming an effective alternative (*85*), with multiplanar reconstruction enabling improved localization and assessment of a variety of lesions. Also, with effective means of monitoring acutely ill patients in the magnetic field, with shorter imaging time, and with the better detection of parenchymal lesions, MRI may play a more active role in the investigation of head trauma. CT underestimates nonhemorrhagic parenchymal injury and frequently does not correlate with the degree of neurologic deficit or with the level of consciousness as assessed by the Glasgow Coma Score (GCS) (*86*). The latter is probably true for MRI as well.

MRI is vastly superior to CT after 48–72 hr posttrauma (in the subacute and chronic phases) for the detection of all intracranial lesions, most especially of nonhemorrhagic primary intra-axial lesions (*83, 84, 86–88*). A recent MRI study categorized these lesions into (a) diffuse axonal injury (DAI), (b) cortical contusion, (c) subcortical gray-matter injury, and (d) brainstem injury (*88*). The most common of these is DAI which results from sheering stresses in the white matter tracts. DAI is multifocal and tends to be associated with more severe initial impairment of consciousness and a poorer prognosis (*83, 87*). Although MRI is superior to CT in detecting DAI, both appear to be quite insensitive in diagnosing these lesions.

CT does not reliably predict the outcome or extent of recovery, in part due to its insensitivity in detecting white matter lesions (*86*). Conversely, the higher sensitivity of MRI may lead to improved predictors of prognosis (*83, 85, 87*).

The literature on PET in head trauma is limited. FDG-PET does not differentiate structural lesions from parenchymal dysfunction, all of which are manifested as reduced glucose metabolism (*89*). Functional changes may extend beyond anatomic abnormalities on CT or MRI (*89, 90*), and are often present in areas adjacent to and remote from the focal damage. Cortical contusion, intracranial hematoma and resultant encephalomalacia tend to have associated metabolic effects that are confined to the site and extent of the anatomic lesion as seen on MRI or CT. However, subdural and epidural hematomas cause widespread hypometabolism, not infrequently involving the contralateral cerebral hemisphere, even when CT and MRI are unremarkable in these regions (*91*) (Fig. 8). DAI can result in widespread cortical hypometabolism, but a striking finding is of profound hypometabolism in the visual cortex (*92*), normally one of the most metabolically active regions. Preliminary work in our laboratory suggests that supratentorial lesions with head injury can cause cerebellar hypometabolism in both the ipsi- and contralateral sides (Fig. 9).

There is correlation with the severity of head trauma, the GCS, and the degree of whole brain hypometabolism (*90*). Global and regional metabolic rates tend to improve along with clinical recovery (*90, 91*). DAI-induced cortical hypometabolism has shown improvement as early as 3 wk on serial PET scans (*91*). Severely injured areas show persistent hypometabolism.

One study suggests that PET, but not CT, correlates closely with neuropsychologic (NP) and language testing in the assessment of site and extent of cerebral dysfunction with possible ramifications for rehabilita-

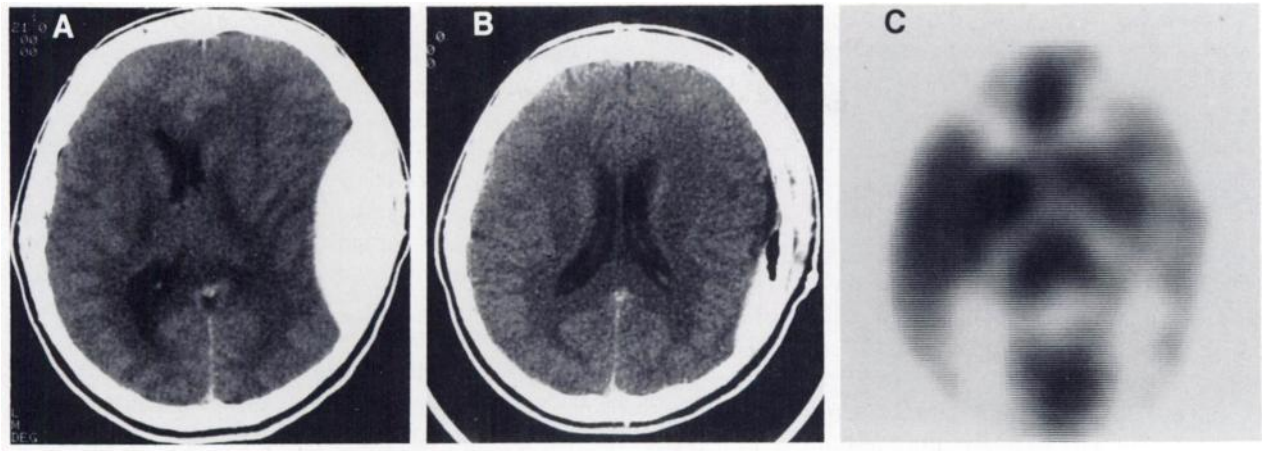

FIGURE 8
A 45-year-old patient who was involved in a motor vehicle accident. A: Transaxial CT demonstrates a large epidural hematoma in the left temporal parietal region at the time of presentation. B: A repeat CT scan 4 days later following surgical decompression demonstrates marked reduction in both the size of the epidural hematoma and mass effect. C: FDG-PET at the time of the repeat CT scan shows widespread left hemispheric hypometabolism which is disproportionately larger than the original size of the anatomic lesion seen on CT.

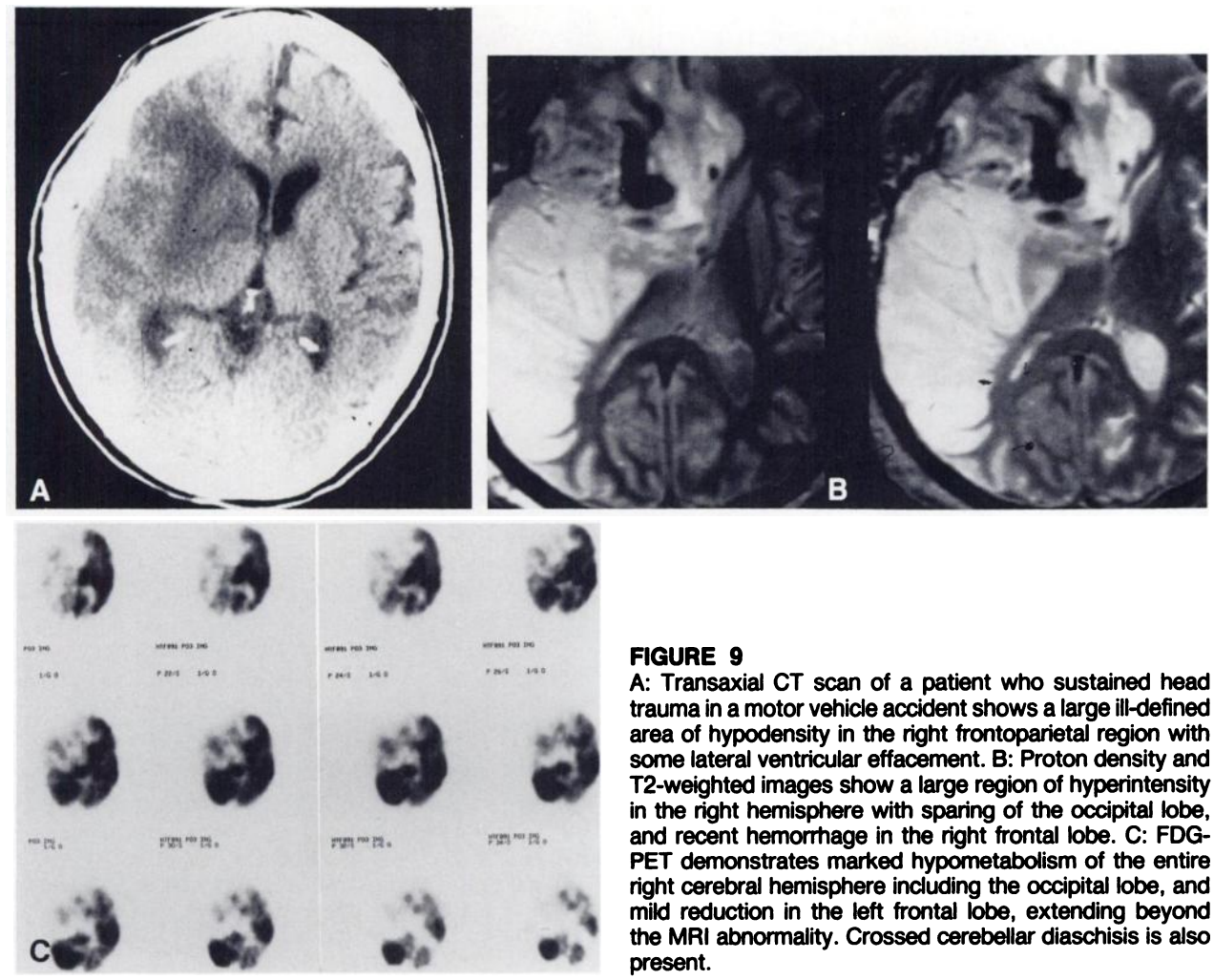

FIGURE 9
A: Transaxial CT scan of a patient who sustained head trauma in a motor vehicle accident shows a large ill-defined area of hypodensity in the right frontoparietal region with some lateral ventricular effacement. B: Proton density and T2-weighted images show a large region of hyperintensity in the right hemisphere with sparing of the occipital lobe, and recent hemorrhage in the right frontal lobe. C: FDG-PET demonstrates marked hypometabolism of the entire right cerebral hemisphere including the occipital lobe, and mild reduction in the left frontal lobe, extending beyond the MRI abnormality. Crossed cerebellar diaschisis is also present.

tion (*93*). Our preliminary data suggest substantial differences between the sites of dysfunction identified by FDG-PET and NP results. Further prognostic data from PET, MRI and NP testing are required.

SCHIZOPHRENIA

Schizophrenia appears to be a heterogeneous disorder, and this may in part account for the conflicting and various results of many studies of brain morphology and function. Hypotheses of the pathogenesis of schizophrenia are abundant. However, symptoms can be broadly categorized as negative and positive. Positive symptoms tend to be much more responsive to neuroleptic therapy than negative symptoms.

Since the first report of ventriculomegaly on CT in schizophrenia (*94*), it has been the most consistent finding in over 90 CT studies of structural abnormalities. Other less frequent abnormalities include global and frontal cortical atrophy and sulcal widening, cerebellar atrophy, cerebral asymmetry, third ventricular dilatation, decreased cranial size and altered brain density when compared with normal controls. These have been variably correlated with prognosis and preponderance of positive or negative symptoms (*95*, *96*). The poor specificity and low frequency (3–40%) (*96*, *97*) of ventriculomegaly has not warranted routine CT examination in suspected schizophrenic patients.

Ventriculomegaly does occur in young, first episode patients (*97*) and tends not to progress as would be expected in a degenerative process such as dementia (*95*). These raise questions as to the onset of the pathological process and temporal relationship to clinical manifestations, and to the possibility of the disorder resulting from a "static lesion" early in brain development (*98*).

Published studies of brain morphologic abnormalities on MRI are difficult to compare because of methodologic differences. As with CT, lateral ventricular dilatation has been noted with MRI (*95*, *99*). The better resolution of MRI has enabled detection of corpus callosal abnormalities, with both increased and decreased size being reported (*99*). This is relevant as failure of interhemispheric communication occurs in some schizophrenics (*100*). As with CT, no consistent focal structural abnormality has been detected to account for the ventriculomegaly (*95*). This may suggest a generalized process or that the resolution of MRI may still be inadequate to detect small regions of atrophy, such as in the medial limbic structures, as has recently been described in neuropathologic studies (*101*).

FDG-PET is employed on the assumption that aberrant neuronal activity will be manifested as abnormal glucose metabolism. FDG-PET studies have demonstrated conflicting results. The two most frequent findings are (a) frontal lobe hypometabolism (hypofrontality) (*102–105*), and (b) relative basal ganglia hypermetabolism (*105–107*), with increased subcortical to cortical ratios reflecting preservation of activity in subcortical structures relative to decreased cortical metabolism (*106*) (Fig. 10). Blood flow studies using $H_2{}^{15}O$ have also demonstrated increased flow to the left globus pallidus (*108*). Other findings include left hemisphere hypometabolism, temporal lobe hypometabolism (*105*), and a normal anterior to posterior gradient. In such studies patient populations, neuropsychological assessment and absence or chronicity of medication are not necessarily uniform. Furthermore, assessment of local cerebral glucose metabolic rates has tended not to consider volume averaging effects because of the proximity of basal ganglia to lateral ventricles or of cortex to widened sulci. Short term neuroleptic treatment tends not to significantly change either the relative hypofrontality (*105*) or the subcortical to cortical ratio (*106*, *109*), but does increase global metabolic rates (*105*). Hypofrontality may relate to chronicity of illness or medications (*103*, *104*).

The concept of hypofrontality is consistent with the hypothesis of frontal lobe dysfunction (*97*, *105*). The frontal cortex is believed to be important for the highest integrative, adaptive, and executive functions. Frontal lobe dysfunction could account for the prominence of negative symptoms (*97*, *105*). Furthermore, FDG-PET studies with specific frontal activation tests of sustained attention by continuous performance tasks, have demonstrated reduced activation of the frontal lobe (*97*, *104*, *110*). In one study, the degree of accentuation of hypofrontality correlated with the preponderance of negative, rather than positive, symptoms (*104*). However, some recent studies have not documented hypofrontality (*111*).

In most patients positive and negative symptoms occur simultaneously. It has been suggested that the

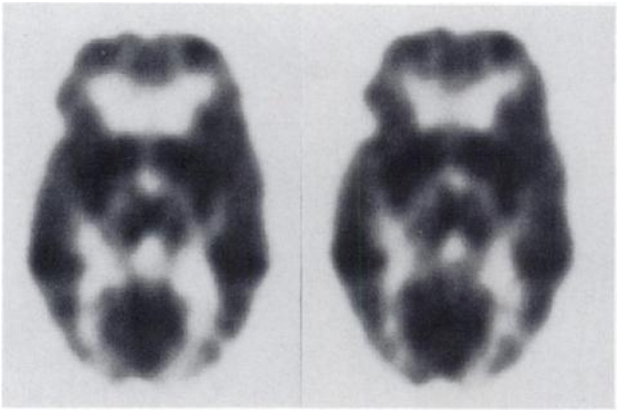

FIGURE 10
FDG-PET in a young patient with schizophrenia shows a relative striatal hypermetabolism, and increased striatal to cortical ratio. The entire cortex appears to be uniformly affected by the underlying process.

temporal and frontal lobes, together with their dopaminergic interconnections through the basal ganglia, be considered a neurobehavioral unit, and that dysfunction of this unit may be involved in the positive symptoms of schizophrenia (*105*). Frontal lobe dysfunction would not only lead to therapy-resistant negative symptoms, but to overaction of subcortical and limbic dopaminergic systems that are normally modulated by the frontal cortex, resulting in positive symptoms (*112*), sensitive to neuroleptics. This may be the basis for the various findings of hypofrontality and relative basal ganglia hypermetabolism seen in FDG-PET studies.

Anatomic and metabolic studies have not unravelled the pathophysiology of schizophrenia. Validation of theories, such as the above, will require in vivo studies of neurotransmitter systems. This is an exciting area of great potential for PET research.

Pharmacologic and neuropathologic studies have implicated the dopamine system in the pathogenesis of schizophrenia, the so-called "dopamine hypothesis". Neuroleptics cause D_2 receptor blockage proportional to antipsychotic efficacy, and amphetamines, which elevate synaptic dopamine levels, induce a schizophreniform psychosis and exacerbate symptoms in schizophrenia. Post-mortem studies have shown a bimodal pattern of D_2 receptor density in brains of schizophrenics, with half of the subjects having normal and half having increased densities (*113*) in the caudate nucleus, putamen and nucleus accumbens. D_1 receptor numbers have remained normal. Controversy exists as to whether the increase in D_2 receptor binding and density results from an adaptation to chronic neuroleptic blockade or from an intrinsic biochemical defect. Post-mortem studies of drug-free or naive patients have shown increased D_2 receptor binding (*114*).

Several agents have been reported for the imaging of CNS D_2 receptors, including butyrophenone derivatives, 3-N-(^{11}C) methyl spiperone ([^{11}C]NMSP), and [^{18}F]NMSP, and the benzamide, [^{11}C]raclopride. Studies on patients undergoing therapy show suppression of striatal radioligand uptake and affinity, which is inversely related to antipsychotic therapy dose and plasma level (*115*). A debate currently exists about the striatal D_2 receptor density in drug-naive schizophrenics. Increased density was found using [^{11}C]NMSP [This occurred not only in drug-naive but in previously treated but drug-free patients (*116*)]. However, using [^{11}C]raclopride the receptor density was normal (*117*). (^{11}C)NMSP is less specific, having some serotonin receptor activity, and binds irreversibly to D_2 receptors. It is possible that [^{11}C]raclopride, which binds reversibly and dissociates rapidly, may be more subject to competition from endogenous dopamine, which is significantly elevated in actively psychotic schizophrenics (*118*). Elevated striatal D_2 receptor density has been reported in other psychotic affective disorders, but not in nonpsychotic affective illnesses (*119*). If further studies confirm a definite increase in D_2 receptor density, this will significantly affect future research.

Although experience is limited to date, neuroreceptor/neurotransmitter imaging and the evaluation of the effects of drugs on regional brain function and chemistry should increase in importance, and facilitate in vivo testing of neurophysiologic theories of schizophrenia and other psychiatric disorders.

MOVEMENT DISORDERS

Huntington's Disease

Huntington's disease (HD) is a lethal neurodegenerative disease of the caudate and putamen, of autosomal dominant inheritance with onset usually in the third through fourth decades, and characterized by progressive chorea and dementia. Recently, an abnormality of the short arm of chromosome 4 has been described (*120*).

CT and MRI identify the pathologically described changes of atrophy of the caudate nuclei, appearing as loss of convexity of the lateral aspect of the adjacent lateral ventricle (*121*, *122*). With progression of dementia and with disease duration, generalized cerebral atrophy becomes worse (*121*, *122*). FDG-PET demonstrates hypometabolism of the caudate and putamen nuclei in all symptomatic subjects (*123*, *126*). In contrast to AD, global and local cortical metabolic rates are normal, and are independent of disease severity, duration, and medications (*124*).

There is debate as to whether PET can detect asymptomatic HD carriers. In two series of at-risk subjects, striatal hypometabolism preceded the onset of symptoms and CT changes (*123–125*). Clinical follow-up has shown that four of 18 (*123*) and one of three (*125*) such subjects with striatal hypometabolism, but none with normal metabolism, have with time developed symptomatic HD. More protracted follow-up is required. It does appear that an abnormal FDG-PET scan could indicate that the subject may be presymptomatic for some undefined period. A normal FDG-PET scan would suggest either that the subject is not an HD heterozygote or that clinical manifestation may be at least some years away (*125*). However, another study could not demonstrate caudate hypometabolism in any at-risk individual (*126*).

In a study of FDG-PET and a polymorphic human linked DNA marker (D4S10), in seven of 13 at-risk subjects there was concordance of these two tests in the indication of either a high or low risk of developing HD. Five subjects had abnormal DNA results and normal PET, and one subject had the reserve. This study suggests that FDG-PET may be useful to confirm abnormal DNA studies, to check for the possibility of

an erroneously abnormal DNA test because of DNA recombination, or to suggest that there may be an undefined period, perhaps years, before symptoms begin if PET is normal and DNA results are abnormal (*125*).

Striatal glucose hypometabolism is not entirely specific for HD, occurring in hereditary chorea and Lesch-Nyhan syndrome. Therefore, DNA and PET studies are complementary in evaluating at-risk individuals for HD (*125*).

D_2 receptor binding studies with (^{11}C)NMSP have demonstrated a reduced D_2 receptor density in the basal ganglia of patients with HD (*127–129*), consistent with postmortem autoradiographic findings (*127*).

Parkinson's Disease

Parkinson's disease (PD) was the first illness in which an abnormality of a neurotransmitter was established. PD is characterized by the triad of bradykinesia, tremor and rigidity with progression to dementia in 20–30% of patients. There is loss of pigmented neurons in the substantia nigra of midbrain and locus coerulus of pons with reduced production of dopamine from decarboxylation of dopa, reduced storage of dopamine, and nigrostriatal system dysfunction. It has been hypothesized that early in PD this denervation is associated with a hypersensitivity due to "upregulation" of striatal dopamine receptors (*130*) and that down regulation may occur as the disease progresses.

CT has little role in PD, detecting no specific striatal abnormality and occasionally only mild, nonspecific ventricular, and sulcal enlargement. The major feature of PD on MRI appears to be a decrease in the width of the pars compacta of the substantia nigra, probably reflecting loss of pigmented cells, but possibly due to iron deposition (*131*). Moderate or marked cortical atrophy tends to occur more frequently than in controls. In parkinsonian-like syndromes MRI shows abnormal intensities in the putamen and to a lesser degree in the caudate nuclei and substantia nigra, suggestive of iron deposition (*132*). Iron is present in many enzyme systems, and deposition may reflect changes in these systems with pathology or age.

As the synapse is a site of significant glucose utilization, nigrostriatal atrophy may be expected to cause reduction in local striatal glucose metabolic rates. Conversely, in the early untreated state mild basal ganglia hypermetabolism has been reported (*133*), and in hemiparkinsonism, hypermetabolism of the basal ganglia contralateral to the symptomatic side has been seen (*134*). Another group detected no significant striatal change (*124*, *135*). Levodopa therapy does not alter local or global metabolic rates (*133*, *135*), despite significant clinical improvement. PD patients tend to have mild, uniform cerebral hypometabolism (average 18% decrease), which worsens with the severity of bradykinesia and development of mild to moderate dementia (*133*). The mechanism of the mild diffuse cortical hypometabolism, which is unrelated to disease duration, is unclear (*133*). Severe dementia of PD may have an FDG-PET appearance indistinguishable from AD with selective parietal hypometabolism (*133*).

Reduced striatal dopamine concentrations result from decreased synthesis from dopa and decreased storage. As would be expected, PET with ^{18}F dopa in PD demonstrates reduced basal ganglia activity especially in patients with the "on/off" phenomenon (*136*). In hemiparkinsonism, there is predominant reduction in the contralateral striatum, but also some irregular reduction in the ipsilateral side (*137*).

Nomifensine is a potent inhibitor of presynaptic dopamine and norepinephrine reuptake sites. In normality, the highest regional brain uptake occurs in the striatal dopaminergic nerve terminals of the nigrostriatal pathway and in the norepinephrine uptake sites in the thalamus (*136*). There is an age-dependent decline (*138*). In PD, striatal uptake of ^{11}C nomifensine is markedly reduced in patients less than 65 yr of age. Older PD patients have striatal binding similar to older controls. In hemiparkinsonism there is reduced bilateral striatal uptake, especially on the side contralateral to symptoms (*138*). Development of an ^{11}C nomifensine enantiomer would refine this technique.

Consistent with the post-synaptic supersensitivity theory, PET with [^{11}C]NMSP suggested a mild increase in binding in early disease, and decreased binding in advanced disease, consistent with subsequent down-regulation (*127*). Patients with hemiparkinsonism have demonstrated bilateral variability in striatal uptake (*127*, *139*).

Treatment with dopaminergic medication would be expected to decrease [^{11}C]NMSP binding in the basal ganglia because of competition with therapy-induced dopamine, down-regulation of the dopamine receptor with therapy, and because of decreased receptor numbers with age. Surprisingly, one group found a bilateral increase in receptor binding following therapy, suggesting either persistent post-synaptic D_2 receptor hypersensitivity, or an alteration in local pharmacokinetics (*139*).

Exposure to the "designer heroin", 1-methyl-4-phenyl 1,2,3,6-tetrahydropyridine (MPTP), can cause an acute parkinsonism. MPTP exposed monkeys and humans demonstrate reduced striatal ^{18}F dopa uptake (*140*, *141*), and marked up-regulation of D_2 receptors using [^{11}C]raclopride (*142*) and [^{18}F]NMSP (*143*). The changes seen in MPTP subjects are more marked than in PD. However, MPTP animals may serve as a useful model for study of PD.

Although much is known about the biochemical abnormalities of PD, the functional problems in the basal ganglia remain unclear. In vivo neurotransmitter

studies should aid in the understanding of PD and assessment of therapy, such as the use of caudate implants.

EPILEPSY

The epilepsies are a heterogeneous group of disorders constituting, as a group, one of the more common serious neurologic illnesses. Not all patients with generalized (GS) or partial seizures (PS) can be controlled with medical therapy. Intractable complex PS can be cured by surgery in appropriately selected candidates. The preoperative localization of the ictal focus entails multiple investigations including FDG-PET, electroencephalography (EEG), CT, and MRI.

PS most frequently originate from a structural lesion in the temporal lobe, resulting in a complex constellation of psychomotor phenomena. The most common pathology is mesial temporal sclerosis (MTS) in which there are one or more foci of neuronal loss and gliosis, involving the hippocampus, dentate, subiculum and amygdala (*144*). Occasionally, tumors, vascular malformations or tuberous sclerosis are the cause.

CT has a limited role, being particularly hampered in the temporal lobe by bone artifact, but will detect larger tumors (*145–148*). MRI affords better resolution and parenchymal resolution without bone artifact. MRI is very sensitive in the detection of nonsclerotic lesions, but has been reported as being poor in detecting MTS, being normal in a series of 18 patients with MTS (*148*). In another series, only one of 14 patients with pathologically confirmed MTS had focal MRI signal abnormalities (*149*) (Fig. 11). Atrophy, as determined by gross asymmetry, sulcal and temporal horn enlargement, occurs more frequently (*150*). These changes may not always correlate with pathologic evidence of MTS (*149*).

EEG is vital in the diagnosis and classification of epilepsy, and in the preoperative localization of the epileptogenic focus. Scalp EEG detects primarily cortical activity and, having low spatial resolution, cannot differentiate primary cortical activity from that propagated from another site. Stereotactically implanted depth electrodes improve localization, but are clearly invasive and therefore have sampling limitations.

Since the calculation of metabolic rates requires steady state conditions for 30–40 min following injection before equilibrium is attained, FDG-PET has poor temporal resolution of changes in glucose metabolism. Thus, any transient metabolic changes, as occur with a seizure, will be averaged with the pre and postictal metabolic rates. Furthermore, the onset of a PS may be unpredictable. Therefore, most FDG-PET studies are performed in the interictal phase. The most consistent finding, occurring in ~70% of PS patients, is of one or more foci of hypometabolism in the region of the primary epileptogenic focus or foci (*151*).

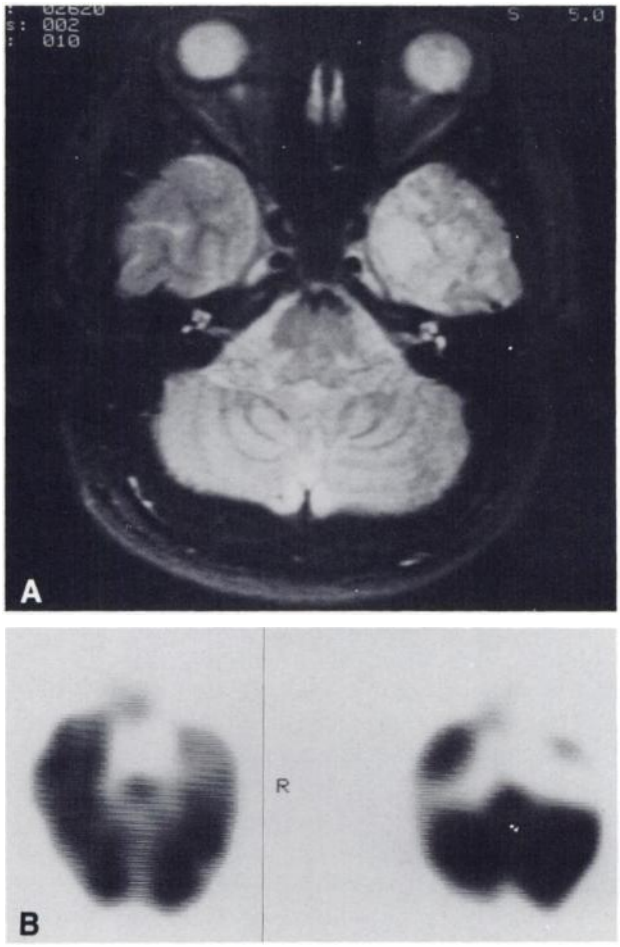

FIGURE 11
A: Transaxial MR image in a patient with complex partial seizures shows focal hyperintensities consistent with mesial temporal sclerosis. B: Interictal FDG-PET scan shows left temporal hypometabolism in an area larger than that seen on MRI.

The extent to which the interictal hypometabolic focus represents the anatomic abnormality and/or functional derangement of metabolism is not entirely clear, but it probably more represents the latter. Such a focus usually involves the mesial temporal lobe and may extend to the entire lobe, to the frontal or parietal lobes, or to the ipsilateral hemisphere. There is individual variation of size and shape of the zone.

The degree of hypometabolism does not correlate with the frequency of EEG spike activity (*151*, *152*), nor with seizure frequency or severity (*152*). PET and EEG appear to measure different aspects of cerebral dysfunction.

In localizing the seizure focus, there was poor correlation when PET was compared with scalp and depth EEG separately. When combined EEG data were compared with PET, the correlation was good, with both localizing the focus in ~70% of patients (*153*). When the EEG focus was unilateral and well defined, there was good correlation between PET and scalp and sphen-

oidal EEG. Diffuse or shifting EEG abnormalities were usually associated with normal PET studies (*154*). Both PET and EEG can cause false positive localization in terms of histological findings (*144*). The very presence of depth electrodes in situ during PET may cause foci of hypometabolism (*144*). PET has better spatial resolution than EEG (*155*), but the zone of hypometabolism may at times be larger than the region suggested by EEG (*152*).

MRI is clearly superior to PET in detecting nonsclerotic structural lesions that cause seizures (*148*). PET appears to be superior to MRI in the detection of MTS. In the abovementioned series, of 18 patients with normal MRI, 56% had temporal lobe hypometabolism (*148*). However, hypometabolism cannot specify histopathology.

The extent of hypometabolism is generally larger than the structural abnormality on histopathology of the resected specimen (*144*). This suggests a functional inhibition of adjacent neuronal elements (*144*). Furthermore, these functional changes appear to be, in part, reversible. During a seizure the hypometabolic zone may become hypermetabolic (*155*). Hypometabolic regions in a patient with Lennox-Gestaut syndrome normalized following commissurotomy (*156*). Postictal scans may show an increased number of hypometabolic foci when compared to interictal scans (*154*). Therefore, regions of hypometabolism may vary and should not be solely relied upon for localization.

MRI, FDG-PET, and EEG are complementary in foci localization. MRI is the preferable initial imaging investigation, excluding most tumors. Consistent localization by scalp EEG and PET may eliminate the need for depth EEG (*154*).

Ictal FDG-PET is of limited value in PS patients because of poor temporal resolution, averaging of metabolic rates, significant individual variation and the variability of ictus onset. In general, the interictal focus of hypometabolism becomes hypermetabolic during a seizure (*154*, *157*) and may spread to become diffuse. The period of postictal depression is associated with marked hypometabolism.

In patients with epilepsia partialis continua or with multiple frequent seizures, there tends to be widespread hypermetabolism rather than a discrete hypermetabolic focus. The areas of ictal hypermetabolism do not always correspond to sites of interictal hypometabolism (*157*).

The use of the shorter lived positron emitter ^{15}O has not aided localization, as reports of CBF, $CMRO_2$, and OER in interictal and ictal phases have given variable results (*158*, *159*).

Interictal and ictal FDG-PET studies on patients with generalized tonic/clonic and petit mal seizures, except with Lennox-Gastaut syndrome, have failed to lateralize or localize an abnormal focus (*152*). Scans performed during electroconvulsive therapy tend to demonstrate a diffuse hypermetabolism with postictal hypometabolism (*157*). Petit mal seizures were associated with a diffuse increase in cerebral metabolism relative to post-therapy seizure-controlled state (*160*).

With further improvement in spatial resolution with PET and higher Tesla MR instruments the relative contributions of these technologies will become more refined. Much is still to be learnt about the electrophysiological and pathophysiologic significance of the interictal zone of hypometabolism in PS patients.

ACKNOWLEDGMENTS

This work was supported by NIH Grants NS14867-10 and NIH AGO3934-07.

REFERENCES

1. Brody H. Organization of the cerebral cortex. III. A study of aging in the human cerebral cortex. *J Comp Neurol* 1955; 102:511–556.
2. Tomlinson BE, Blessed G, Roth M. Observations on the brains of nondemented old people. *J Neurol Sci* 1968; 7:331–356.
3. Anderson JM, Hubbard BM, Coghill GR, et al. The effect of advanced old age on the neurone content of the cerebral cortex: observations with an automatic image analyser point counting method. *J Neurol Sci* 1983; 58:235–246.
4. Haug G. Age and sex dependence of the size of normal ventricles on computed tomography. *Neuroradiology* 1977; 14:201–204.
5. Zatz LM, Jernigan TL, Ahumada AJ, Jr. Changes on computed cranial tomography with aging: intracranial fluid volume. *AJNR* 1982; 3:1–11.
6. de leon MJ, George AE, Ferris SH, et al. Positron emission tomography and computed tomography assessment of the aging human brain. *JCAT* 1984; 8:88–94.
7. George AE, de Leon MJ, Kalnin A, et al. Leukoencephalopathy in normal and pathologic aging: 2. MRI of brain lucencies. *AJNR* 1986; 7:567–570.
8. Brant-Zawadski M, Fein G, Van Dyke D, et al. MR imaging of the aging brain: Patchy white-matter lesions and dementia. *AJNR* 1985; 6:675–682.
9. George AE, de Leon MJ, Gentes CI, et al. Leukoencephalopathy in normal and pathologic aging: 1. CT of brain lucencies. *AJNR* 1986; 561–566.
10. Braffman BH, Zimmerman RA, Trojanoqski JQ, et al. Brain MR: Pathologic correlation with gross and histopathology. 2. Hyperintense white-matter foci in the elderly. *AJNR* 1988; 9:629–636.
11. Drayer BP, Imaging of the aging brain. Part 1. *Radiology* 1988; 166:785–796.
12. Fazekas F, Chawluk JB, Alavi A, et al. MR signal abnormalities at 1.5 T in Alzheimer's dementia and normal aging. *AJNR* 1987; 8:421–426.
13. Duara R, Margolin RA, Robertson-Tchabo EA, et al. Cerebral glucose utilization as measured with positron emission tomography in 21 resting healthy men between the ages of 21 and 83 years. *Brain* 1983; 106:761–775.
14. deLeon M, George A, Tomanelli J, et al. PET scanning demonstrates that aging in man is accompanied

by loss of integration of regional brain activity without concurrent reduction in absolute regional cerebral metabolic rates for glucose. *J Cereb Blood Flow Metab* 1985; 5:S119.
15. Alavi A. The aging brain. *J Neuropsychiatry* 1989; 1(suppl1):S51–S55.
16. Dastur DK. Cerebral blood flow and metabolism in normal human aging, pathological aging, and senile dementia. *J Cereb Blood Flow Metab* 1985; 5:1–9.
17. Kuhl DE, Metter EJ, Rieger WH, Phelps ME. Effects of human aging on patterns of local cerebral glucose utilization determined by the [^{18}F]fluorodeoxyglucose method. *J Cereb Blood Flow Metab* 1982; 2:163–171.
18. Chawluk JB, Alavi A, Jamieson DG, et al. Changes in local cerebral glucose metabolism with normal aging, the effects of cardiovascular and systemic health factors. *J Cereb Blood Flow Metab* 1987; 7(suppl 1):S411.
19. de Leon M, George A, Tomanelli J, et al. Positron emission tomography studies of normal aging, a replication of PET III and 18-FDG using PET VI and II-CDG. *Neurobiol Aging* 1987; 8:319–323.
20. Chawluk J, Alavi A, Hurtig H, et al. Altered patterns of regional cerebral glucose metabolism in aging and dementia. *J Cereb Blood Flow Metab* 1985; 5(suppl 1):S121–S122.
21. Alavi A, Dann R, Chawluk J, et al. Positron emission tomography imaging of regional cerebral glucose metabolism. *Semin Nucl Med* 1986; 16:2–34.
22. Sokoloff L. Cerebral circulatory and metabolic changes associated with aging. *Res Publ Assoc Res Nerv Ment Dis* 1966; 41:237–254.
23. Frackowiak RSJ, Wise RJS, Gibbs JM, et al. Positron emission tomographic studies in aging and cerebrovascular disease at Hammersmith Hospital. *Ann Neurol* 1984; 15(suppl):S112–118.
24. Pantano P, Baron JC, Lebrum-Grandie P, et al. Regional cerebral blood flow and oxygen consumption in human aging. *Stroke* 1984; 15:635–641.
25. Frackowiak RSJ, Lenzi GL, Jones T, et al. Quantitative measurement of regional cerebral blood flow and oxygen metabolism in man using 150 and positron emission tomography; theory, procedure and normal values. *JCAT* 1980; 4:727–736.
26. Yamaguchi T, Kanno I, Uemura K, et al. Reduction in regional cerebral metabolic rate of oxygen during human aging. *Stroke* 1986; 17:1220–1228.
27. Beck JC, Benson DF, Scheibel AB, et al. Dementia in the elderly: the silent epidemic. *Ann Intern Med* 1982; 97:231–241.
28. Jellinger K. Neuropathological aspects of dementia resulting from abnormal blood and cerebrospinal fluid dynamics. *Acta Neurol Belg* 1976; 76:83–102.
29. Ho DD, Rota TR, Schooley RT, et al. Isolation of HTLV-III from cerebrospinal fluid and neural tissues of patients with neurologic syndromes related to the acquired immunodeficiency syndrome. *N Engl J Med* 1985; 313:1493–1497.
30. Tomlinson BE, Blessed G, Roth M. Observations on the brains of demented old people. *J Neurol Sci* 1970; 11:205–242.
31. Gado MH, Hughes CP, Danziger W, et al. Volumetric measurements of the cerebrospinal fluid spaces in subjects with dementia and in controls. *Radiology* 1982; 144:535–538.
32. Albert M, Naeser MA, Levine HL, et al. Ventricular size in patients with presenile dementia of the Alzheimer type. *Arch Neurol* 1984; 41:1258–1263.
33. Damasio H, Eslinger P, Damasio AR, et al. Quantitative computed tomography analysis in the diagnosis of dementia. *Arch Neurol* 1983; 40:715–719.
34. George AE, Stylopoulos LA, de Leon MJ, et al. Temporal lobe CT diagnostic features of Alzheimer's disease [Abstract]. Presented at the 25th Annual Meeting of the ASNR, New York, May 1987. *AJNR* 1987; 8:931.
35. Pettegrew JW, Moossy J, Withers G, et al. 31-P nuclear magnetic resonance study of the brain in Alzheimer's disease. *J Neuropathol Exp Neurol* 1988; 47:235–248.
36. Pettegrew JW, Koop SJ, Minshew NJ, et al. 31-P nuclear magnetic resonance studies of phosphoglyceride metabolism in developing and degenerating brain: Preliminary observations. *J Neuropathol Exp Neurol* 1987; 6:419–430.
37. Alavi A, Lenkinski R, Chawluk J, et al. Correlation of positron emission tomography (PET) and magnetic resonance spectroscopy (MRS) in CNS disorders [Abstract]. *J Nucl Med* 1988; 29:910.
38. Duara R, Grady C, Haxby J, et al. Positron emission tomography in Alzheimer's disease. *Neurology* 1986; 36:879–887.
39. Alavi A, Chawluk J, Hurtig H, et al. Determination of patterns of regional cerebral glucose metabolism in normal aging and dementia [Abstract]. *J Nucl Med* 1985; 26:P69.
40. Alavi A, Jolles PR, Jamieson DG, et al. Anatomical and functional changes of the brain in normal aging and dementia as demonstrated by MRI, CT, and PET. *Nucl Med Ann* 1989: 49–79.
41. Frackowiak RSJ, Pozzilli C, Legg NJ, et al. Regional cerebral oxygen supply and utilization in dementia: a clinical and physiological study with oxygen-15 and positron tomography. *Brain* 1981; 104:753–778.
42. Frackowiak RSJ, Pozzilli C, Legg NJ, et al. A prospective study of regional cerebral blood flow and oxygen utilization in dementia using positron emission tomography and oxygen-15. *J Cereb Blood Flow Metab* 1981; 1:S453–S454.
43. Jamieson DG, Chawluk JB, Alavi A, et al. The effect of disease severity on local cerebral glucose metabolism in Alzheimer's disease. *J Cereb Blood Flow Metab* 1987; 7(supp 1):S410.
44. Benson F, Kuhl DE, Hawkins ME, et al. The fluorodeoxyglucose ^{128}F scan in Alzheimer's disease and multi-infarct dementia. *Arch Neurol* 1983; 40:711.
45. Kamo H, McGeer R, Harrop R, et al. Positron emission tomography and histopathology in Pick's disease. *Neurology* 1987; 37:439.
46. Chawluk JB, Alavi A, Dann R, et al. Positron emission tomography in aging and dementia: effect of cerebral atrophy. *J Nucl Med* 1987; 28:431–437.
47. Bradley WG, Jr, Waluch V, Yadley RA, et al. Comparison of CT and MR in 400 patients with suspected disease of the brain and cervical spinal cord. *Radiology* 1984; 152:695–702.
48. Kucharczyk W, Brant-Zawadski M, Sobel D, et al. Central nervous system tumors in children: detection by magnetic resonance imaging. *Radiology* 1985; 155:131–136.
49. Felix R, Schorner W, Laniado M, et al. Brain tumors: MR imaging with gadolinium-DTPA. *Radiology* 1985; 156:681–688.

50. Kelly WM, Brant-Zawadski M. Magnetic resonance imaging and computed tomography of supratentorial tumors. In: Taveras JM, Ferrucci JT, eds. Philadelphia: *Radiology: diagnosis-imaging-intervention.* Chap 53. J.P. Lippincott. 1988:1–21.
51. Hesselink JR, Press GA. MR contrast enhancement of intracranial lesions with Gd-DTPA. *Radiol Clin North Am* 1988; 26:873–887.
52. Brant-Zawadski M, Davis PL, Crooks LE, et al. NMR demonstration of cerebral abnormalities: comparison with CT. *Am J Roentgenol* 1983; 140:847.
53. Brant-Zawadski M, Badami JP, Mills CM, et al. Primary intracranial tumor imaging: a comparison of magnetic resonance and CT. *Radiology* 1984; 150:435–440.
54. Dooms GC, Hecht S, Brant-Zawadski M, et al. Brain radiation lesions: MR imaging. *Radiology* 1986; 158:149–155.
55. Wrenn FR, Good ML, Handler P. The use of positron emitting radioisotopes for the localization of brain tumors. *Science* 1951; 113:525–527.
56. O'Tuama LA. Methionine transport in brain tumors. *J Neuropsychiatry* 1989; 1(suppl 1):S37–S44.
57. Hiesiger E, Logan J, Wolf AP, et al. Serial PET studies of human cerebral malignancy with [1-^{11}C] putrescine (11C-PUT) and [1-^{11}C]2-deoxy-D-glucose (^{11}C-2DG) [Abstract]. *J Nucl Med* 1986; 27:889.
58. Di Chiro G. Positron emission tomography using [^{18}F] fluorodeoxyglucose in brain tumors. A powerful diagnostic and prognostic tool. *Invest Radiol* 1986; 22:360–371.
59. Di Chiro G, DeLaPaz RL, Brooks RA, et al. Glucose utilization of cerebral gliomas measured by ^{18}F fluorodeoxyglucose and positron emission tomography. *Neurology* 1982; 32:1323–1329.
60. Patronas NJ, Brooks RA, DeLaPaz RL, et al. Glycolytic rate (PET) and contrast enhancement (CT) in human cerebral gliomas. *AJNR* 1983; 533–535.
61. Alavi J, Alavi A, Dann R, et al. Metabolic brain imaging correlated with clinical features and brain tumors [Abstract]. *J Nucl Med* 1985; 18:P64.
62. Alavi JB, Alavi A, Chawluk J, et al. Positron emission tomography in patients with glioma. A predictor of prognosis. *Cancer* 1988; 62:1074–1078.
63. Kushner M, Tobin M, Alavi A, et al. Cerebellar glucose consumption in normal and pathologic states using fluorine-FDG and PET. *J Nucl Med* 1987; 28:1667–1670.
64. Baron JC, Bousser MG, Comar D. Crossed cerebellar diaschisis; a remote functional depression secondary to supratentorial infarction in man. *J Cereb Blood Flow Metab* 1981; 1(suppl 1):S500–S501.
65. Alavi JB, Alavi A, Powe J, Hackney D, Reivich M. Metabolic and structural findings related to white matter disorders as shown by PET, MRI and CT [Abstract]. *J Nucl Med* 1986; 27:899.
66. Doyle WK, Budinger TF, Valk PE, et al. Differentiation of cerebral radiation necrosis from tumor recurrence by [^{18}F]FDG and ^{82}Rb positron emission tomography. *JCAT* 1987; 11:563–570.
67. Patronas NJ, Di Chiro G, Brooks RA, et al. Work in progress: (18F) fluorodeoxyglucose and positron emission tomography in the evaluation of radiation necrosis of the brain. *Radiology* 1982; 144:885–889.
68. Schad LR, Boesecke R, Schlegel W, et al. Three dimensional correlation of CT, MR, and PET studies in radiotherapy treatment planning of brain tumors. *JCAT* 1987; 11:948–954.
69. Wang A-M, Lin JC-T, Rumbaugh CL. What is expected of CT in the evaluation of a stroke? *Neuroradiol* 1988; 30:54–58.
70. Pressman BD, Tourje EJ, Thompson JR. An early sign of ischemic infarction: increased density in a cerebral artery. *AJNR* 1987; 8:645–648.
71. Shih TTF, Huang K-M. Acute stroke: detection of changes in cerebral perfusion with dynamic CT scanning. *Radiology* 1988; 169:469–474.
72. Tomura N, Uemura K, Inugami A, et al. Early CT finding in cerebral infarction: obscuration of the lentiform nucleus. *Radiology* 1988; 168:463–467.
73. Spetzler RF, Zabramski JM, Kaufman B, et al. Acute NMR changes during MCA occlusion: a preliminary study in primates. *Stroke* 1983; 14:185–190.
74. Kushner M, Reivich M, Fieschi C, et al. Metabolic and clinical correlates of acute ischemic infarction. *Neurology* 1987; 37:1103–1110.
75. Kuhl DE, Phelps ME, Kowell AP, et al. Effect of stroke on local cerebral metabolism and perfusion: mapping by emission computed tomography of ^{18}FDG and $^{13}NH_3$. *Ann Neurol* 1980; 8:47–60.
76. Lassen NA. The luxury perfusion syndrome and its possible relation to acute metabolic acidosis localized within the brain. *Lancet* 1966; 2:1113–1115.
77. Baron JC, Bousser MG, Rey A, et al. Reversal of focal "misery-perfusion syndrome" by extracranial bypass in hemodynamic cerebral ischemia. *Stroke* 1981; 12:454–459.
78. Ackerman RH, Correia JA, Alpert NM, et al. Positron imaging in ischemic stroke disease using compounds labeled with oxygen 15. *Arch Neurol* 1981; 38:537–543.
79. Frackowiak RSJ, Wise RJS. Positron tomography in ischemic cerebrovascular disease. *Neurologic Clinics* 1983; 1:183–200.
80. Itoh M, Hatazawa J, Pozzilli C, et al. Positron CT imaging of an impending stroke. *Neuroradiol* 1988; 30:276–279.
81. Pappata S, Tran Dinh S, Baron JC, et al. Remote metabolic effects of cerebrovascular lesions: magnetic resonance and positron tomography imaging. *Neuroradiol* 1987; 29:1–6.
82. Welch KMA, Ewing JR, Chopp M, et al. In vivo31-P NMR of adult human brain. *J Cereb Blood Flow Metab* 1985; 5(suppl 1):S591–S592.
83. Kelly AB, Zimmerman RD, Snow RB, et al. Head trauma: comparison of MR and CT-experience in 100 patients. *AJNR* 1988; 9:699–708.
84. Levin HS, Amparo E, Eisenberg HM, et al. Magnetic resonance imaging and computerized tomography in relation to the neurobehavioural sequelae of mild and moderate head injuries. *J Neurosurg* 1987; 66:706–713.
85. Hadley DM, Teasdale GM, Jenkins A, et al. Magnetic resonance imaging in acute head injury. *Clin Radiol* 1988; 39:131–139.
86. Gentry LR, Godersky JC, Thompson B, et al. Prospective comparative study of intermediate-field MR and CT in the evaluation of closed head trauma. *Am J Roentgenol* 1988; 150:673–682.
87. Zimmerman RA, Bilaniuk LT, Hackney DB, et al. Head injury: early results of comparing CT and high-field MR. *Am J Roentgenol* 1986; 147:1215–1222.
88. Gentry LR, Godersky JC, Thompson B. MR imaging of head trauma: review of the distribution and radio-

pathologic features of traumatic lesions. *Am J Roentgenol* 1988; 150:663–672.
89. Langfitt TW, Obrist WD, Alavi A, et al. Computerized tomography, magnetic resonance imaging, and positron emission tomography in the study of brain trauma. Preliminary observations. *J Neurosurg* 1986; 64:760–767.
90. Alavi A, Fazekas T, Alves W, et al. Positron emission tomography in the evaluation of head injury. *J Cereb Blood Flow Metab* 1987; 7(suppl 1):S646.
91. George JK, Alavi A, Zimmerman RA, et al. Metabolic (PET) correlates of anatomic lesions (CT/MRI) produced by head trauma [Abstract]. *J Nucl Med* 1989; 30:802.
92. Alavi A. Functional and anatomic studies of head injury. *J Neuropsychiatry* 1989; 1(suppl 1):S45–50.
93. Rao N, Turski PA, Polcyn RE, et al. ^{18}F positron emission computed tomography in closed head injury. *Arch Phys Med Rehab* 1984; 65:780–785.
94. Johnstone EC, Crowe TJ, Frith CD, et al. Cerebral ventricular size and cognitive impairment in chronic schizophrenia. *Lancet* 1976; 2:924–926.
95. Kelsoe JR, Cadet JL, Pickar D, et al. Quantitative neuroanatomy in schizophrenia. *Arch Gen Psychiatry* 1988; 45:533–541.
96. Pfefferbaum A, Zipursky RB, Lim KO, et al. Computed tomographic evidence for generalised sulcal and ventricular enlargement in schizophrenia. *Arch Gen Psychiatry* 1988; 45:633–640.
97. Anreasen NC. Brain imaging: applications in psychiatry. *Science* 1988; 239:1381–1388.
98. Weinberger DR. Implications of normal brain development for the pathogenesis of schizophrenia. *Arch Gen Psychiatry* 1987; 44:660–669.
99. Rossi A, Stratta P, Gallucci M, et al. Brain morphology in schizophrenia by magnetic resonance imaging (MRI). *Acta Psychiatr Scand* 1988; 77:741–745.
100. Beaumont J, Dimond S. Brain disconnection and schizophrenia. *Br J Psychiatry* 1973; 123:661–662.
101. Bogerts B, Meertz E, Schonfeldt-Bausch R. Basal ganglia and limbic system pathology in schizophrenia. *Arch Gen Psychiatry* 1985; 42:784–791.
102. Buchsbaum MS, Ingvar DH, Kesslar R, et al. Cerebral glucography with positron tomography. *Arch Gen Psychiatry* 1982; 39:251–259.
103. Farkas T, Wolf A, Jaeger J, et al. Regional brain glucose metabolism in chronic schizophrenia. *Arch Gen Psychiatry* 1984; 41:293–300.
104. Volkow ND, Wolf AP, Van Gelder P, et al. Phenomenological correlates of metabolic activity in 18 patients with chronic schizophrenia. *Am J Psychiatry* 1987; 144:151–158.
105. Wolkin A, Jaegar J, Brodie JD, et al. Persistence of cerebral metabolic abnormalities in chronic schizophrenia as determined by positron emission tomography. *Am J Psychiatry* 1985; 142:564–571.
106. Resnick SM, Gur RE, Alavi A, et al. Positron emission tomography and subcortical glucose metabolism in schizophrenia. *Psychiatry Res* 1988; 24:1–11.
107. Gur RE, Resnick SM, Alavi A, et al. Regional brain function in schizophrenia: I. A positron emission tomography study. *Arch Gen Psychiatry* 1987; 44:119–125.
108. Early TS, Reiman EM, Raichle ME, et al. Left globus pallidus abnormality in never-medicated patients with schizophrenia. *Proc Natl Acad Sci USA* 1987; 84:561–563.
109. Gur RE, Resnick SM, Gur RC, et al. Regional brain function in schizophrenia: II. Repeated evaluation with positron emission tomography. *Arch Gen Psychiatry* 1987; 44:126–129.
110. Cohen RM, Semple WE, Gross M, et al. From syndrome to illness: delineating the pathophysiology of schizophrenia with PET. *Schizophr Bull* 1988; 14:169–176.
111. Kling AS, Metter EJ, Riege WH, et al. Comparison of PET measurement of local brain glucose metabolism and CAT measurement of local brain atrophy in chronic schizophrenia and depression. *Am J Psychiatry* 1986; 143:175–180.
112. Bannon MJ, Roth RH. Pharmacology of mesocortical neurons. *Pharmacol Rev* 1983; 35:53–68.
113. Seeman P. Dopamine receptors and the dopamine hypothesis of schizophrenia. *Synapse* 1987; 1:133–152.
114. Owen F, Crow TJ, Poulter M, et al. Increased dopamine receptor sensitivity in schizophrenia. *Lancet* 1978; ii:223–226.
115. Smith M, Wolf AP, Brodie JD, et al. Serial (^{18}F)N-methylspiroperidol PET studies to measure changes in antipsyotic drug D-2 receptor occupancy in schizophrenic patients. *Biol Psychiatry* 1988; 23:653–663.
116. Wong DF, Wagner HN Jr, Tube LE, et al. Positron emission tomography reveals elevated D_2 dopamine receptors in drug-naive schizophrenics. *Science* 1986; 234:1558–1563.
117. Farde L, Wiesel FA, Hall H, et al. No D_2 receptor increase in PET study of schizophrenia. *Arch Gen Psychiatry* 1987; 44:671–672.
118. Seeman P, Guan HC, Niznik HB. Endogenous dopamine lowers the dopamine D_2 receptor density as measured by (^{3}H)raclopride: implications for positron emission tomography of the human brain. *Synapse* 1989; 3:96–97.
119. Pearlson GD, Wong DF, Ross CA, et al. D2 dopamine receptors increased in psychotic, but not non-psychotic affective disorder. The Johns Hopkins Fifth Annual Symposium 1989: PET imaging of brain chemistry.
120. Gusella JF, Wexler NS, Conneally PM, et al. A polymorphic DNA marker genetically linked to Huntington's disease. *Nature* 1983; 306:234–238.
121. Kuhl DE, Phelps ME, Markham CH, et al. Cerebral metabolism and atrophy in Huntington's disease determined by ^{18}FDG and computed tomographic scan. *Ann Neurol* 1982; 12:425–434.
122. Lukes SA, Aminoff MJ, Crooks J, et al. Nuclear magnetic resonance imaging in movement disorders. *Ann Neurol* 1983; 13:690–691.
123. Mazziotta JC, Phelps ME, Pahl JJ, et al. Reduced cerebral glucose metabolism in asymptomatic subjects at risk for Huntington's disease. *N Engl J Med* 1987; 316:357–362.
124. Kuhl DE, Metter EJ, Riege WH, et al. Patterns of cerebral glucose utilization in Parkinson's disease and Huntington's disease. *Ann Neurol* 1984; 15(suppl): S119–S125.
125. Hayden MR, Hewitt J, Stoessl AJ, et al. The combined use of positron emission tomography and DNA polymorphisms for preclinical detection of Huntington's disease. *Neurology* 1987; 37:1441–1447.
126. Young AB, Penney JB, Starosta-Rubinstein S, et al. Normal caudate glucose metabolism in persons at risk for Huntington's disease. *Arch Neurol* 1987;

44:254–257.
127. Hagglund J, Aquilonius S-M, Eckernas S-A, et al. Dopamine receptor properties in Parkinson's disease and Huntington's chorea evaluated by positron emission tomography using ^{11}C-N-methyl-spiperone. *Acta Neurol Scand* 1987; 75:87–94.
128. Wong DF, Links JM, Wagner HN, et al. Dopamine and serotonin receptors measured in vivo in Huntington's disease with c-11-N-methylspiperone PET imaging [Abstract]. *J Nucl Med* 1985; 26:P107.
129. Leenders KL, Frackowiak RSJ, Quinn N, et al. Brain energy metabolism and dopaminergic function in Huntington's disease measured in vivo using positron emission tomography. *Movement Disorders* 1986; 1:69–77.
130. Marsden CD. Basal ganglia disease. *Lancet* 1982; ii:1141–1147.
131. Braffman BH, Grossman RI, Goldberg HI, et al. MR imaging of Parkinson's disease with spin-echo and gradient sequences. *Am J Roentgenol* 1989; 152:159–165.
132. Drayer BP, Olanow W, Burger P, et al. Parkinson plus syndrome diagnosis using high field MR imaging of brain iron. *Radiology* 1986; 159:493–498.
133. Rougemont D, Baron JC, Collard P, et al. Local cerebral glucose utilisation in treated and untreated patients with Parkinson's disease. *J Neurol Neurosurg Psychiatry* 1984; 47:824–830.
134. Martin WRW, Beckman JH, Calne DB, et al. Cerebral glucose metabolism in Parkinson's disease. *Can J Neurol Sci* 1984; 11:169–173.
135. Kuhl DE, Metter EJ, Riege WH. Patterns of local cerebral glucose utilization determined in Parkinson's disease by the {^{18}F}fluorodeoxyglucose method. *Ann Neurol* 1984; 15:419–424.
136. Leenders KL, Palmer AJ, Quinn N, et al. Brain dopamine metabolism in patients with Parkinson's disease measured with positron emission tomography. *J Neurol Neurosurg Psychiatry* 1986; 49:853–860.
137. Garnett ES, Nahmias C, Firnau G. Central dopaminergic pathways in hemiparkinsonism examined by positron emission tomography. *Can J Neurol Sci* 1984; 11:174–179.
138. Tedrroff J, Aquilonius S-M, Hartvig P, et al. Monoamine re-uptake sites in the human brain evaluated by means of ^{11}C-nomifensine and positron emission tomography: the effects of age and Parkinson's disease. *Acta Neurol Scand* 1988; 77:192–201.
139. Wijnand A, Rutgers F, Lakke JPW, et al. Tracing of dopamine receptors in hemiparkinsonism with positron emission tomography (PET). *J Neurol Sci* 1987; 80:237–248.
140. Chiueh CC, Firnau G, Burns RS, et al. Determination and visualization of damage to striatal dopaminergic terminals in 1-methyl-4-phenyl-1,2,3,6-tetrahydropyridine-induced parkinsonism by [^{18}F]-labeled 6-fluoro-L-dopa and positron emission tomography. *Adv Neurol* 1986; 45:167–169.
141. Calne DB, Langston JW, Wayne WR, et al. Positron emission tomography after MPTP: observations relating to the cause of Parkinson's disease. *Nature* 1985; 317:246–248.
142. Leenders KL, Aquilonius S-M, Bergstrom K, et al. Unilateral MPTP lesion in a rhesus monkey: effects on the striatal dopaminergic system measured in vivo with PET using various novel tracers. *Brain Res* 1988; 445:61–67.
143. Perlmutter JS, Kilbourn MR, Raichle ME, et al. MPTP-induced up-regulation of in vivo dopaminergic radioligand-receptor binding in humans. *Neurology* 1987; 37:1575–1579.
144. Engel J Jr, Brown WJ, Kuhl DE, et al. Pathological findings underlying focal temporal lobe hypometabolism in partial epilepsy. *Ann Neurol* 1982; 12:518–528.
145. Blom RJ, Vinuela F, Fox AJ, et al. Computed tomography in temporal lobe epilepsy. *JCAT* 1984; 8:401–405.
146. Latack JT, Abou-Khalil BW, Siegel GJ, et al. Patients with partial seizure: evaluation by MR, CT, and PET imaging. *Radiology* 1986; 159:159–163.
147. Theodore WH, Dorwart R, Holmes M, et al. Neuroimaging in refractory partial seizures. Comparison of PET, CT and MRI. *Neurology* 1986; 36:750–759.
148. Sperling MR, Wilson G, Engel J Jr, et al. Magnetic resonance imaging in intractable partial epilepsy: correlative studies. *Ann Neurol* 1986; 20:57–62.
149. Fobben ES, Zimmerman RA, Sperling MR, et al. MR imaging in temporal lobe epilepsy [Abstract]. *Radiology* 1988; 169(suppl):142.
150. Alavi A, Sperling M, Zimmerman RA, et al. Comparison of positron emission tomography and magnetic resonance imaging in partial epilepsy [Abstract]. *J Nucl Med* 1988; 29:910.
151. Engel J Jr, Kuhl DE, Phelps ME, et al. Interictal cerebral glucose metabolism in partial epilepsy and its relation to EEG changes. *Ann Neurol* 1982; 12:510–517.
152. Theodore WH, Newmark ME, Sato S, et al. (^{18}F)Fluorodeoxyglucose positron emission tomography in refractory complex partial seizures. *Ann Neurol* 1983; 14:429–437.
153. Engel J Jr, Kuhl DE, Phelps ME, et al. Comparative localization of epileptic foci in partial epilepsy by PCT and EEG. *Ann Neurol* 1982; 12:529–537.
154. Abou-Khalil BW, Siegel GJ, Sackellares JC, et al. Positron emission tomography studies of cerebral glucose metabolism in chronic partial epilepsy. *Ann Neurol* 1987; 22:480–486.
155. Engel J Jr. The use of positron emission tomographic scanning in epilepsy. *Ann Neurol* 1984; 15(suppl): S180–S191.
156. Gur RC, Sussman NM, Alavi A, et al. Positron emission tomography in two cases of childhood epileptic encephalopathy (Lennox-Gestaut syndrome). *Neurology* 1982; 32:1191–1194.
157. Engel J Jr, Kuhl DE, Phelps ME. Patterns of human local glucose metabolism during epileptic seizures. *Science* 1982; 218:64–66.
158. Bernardi S, Trimble MR, Frackowick RS, et al. An interictal study of partial epilepsy using positron emission tomography and the O-15 inhalation technique. *J Neurol Neurosurg Psychiatry* 1983; 46:473–477.
159. Franck G, Sadzot B, Salmon E, et al. Regional cerebral blood flow and metabolic rates in human focal epilepsy and status epilepticus. In: Delgrado-Escueta AV, Ward AA Jr, Woodbury DM et al., eds. *Advances in neurology.* Vol 44. New York: Raven Press, 1986:935–948.
160. Engel J Jr, Lubens P, Kuhl D, et al. Local cerebral metabolic rate for glucose during petit mal absences. *Ann Neurol* 1985; 17:121–128.